

Cooperative Formation of Chiral Patterns during Growth of Bacterial Colonies

Eshel Ben-Jacob, Inon Cohen, Ofer Shochet, and Adam Tenenbaum

*School of Physics and Astronomy, Raymond and Beverly Sackler Faculty of Exact Sciences,
Tel Aviv University, Tel Aviv 69978, Israel*

András Czirók and Tamás Vicsek

Department of Atomic Physics, Eötvös University, Budapest, Puskin u 5-7, 1088 Hungary

(Received 28 September 1994)

Bacterial colonies can develop chiral morphology in which the colony consists of twisted branches, all with the same handedness. Microscopic observations of the chiral growth are presented. We propose that the observed (macroscopic) chirality results from the microscopic chirality of the flagella (via handedness in tumbling) together with orientation interaction between the bacteria. The above assumptions are tested using a generalized version of the communicating walkers model.

PACS numbers: 87.10.+e, 61.43.Hv

Efficient adaptation of bacterial colonies to adverse growth conditions requires cooperative behavior and self-organization. This is done via several communications channels [1–8], from direct (by contact) bacterium-bacterium physical and chemical interaction to indirect interactions via marks left on the agar surface and chemotactic signaling. For researchers in pattern formation, the above communication, regulation, and control mechanisms open a new class of challenging complex models.

Much attention has been given to growth of bacterial colonies on low-nutrient, semisolid agar [9–20]. The colonies adopt various shapes as growth conditions are varied, from compact patterns at high nutrient levels to fractal and dense-branching patterns at low nutrient levels [see Fig. 1(a) for an example of branching growth].

Optical microscope observations reveal that the \mathcal{T} morphotype bacteria perform a random-walk-like movement within a well defined envelope of a “lubrication” layer [14]. [The term morphotype refers to the inheritable geometrical (morphological) character of the colony that can

be transferred by an individual bacterium. The terminology was suggested by D. Gutnick. \mathcal{T} morphotype refers to the bacteria that exhibit tip-splitting (branching) growth. Ben-Jacob *et al.* have derived the \mathcal{T} morphotype from *Bacillus subtilis* 168 grown on low nutrient substrate [16,18].] The latter is formed presumably by chemicals that are excreted by the bacteria and/or by fluid drawn by the bacteria from the agar. The envelope propagates slowly, as if by the action of effective internal pressure produced by the collective movement of the bacteria. Hence, both the envelope formation and the propagation reflect cooperative behavior of the bacteria.

During growth of \mathcal{T} morphotype on a soft substrate (about 1% agar concentration) bursts of new patterns that overgrow the original branching pattern are observed [Fig. 1(b)]. The new patterns consist of thinner branches, all with the same handedness of strong twisting (free branches can twist more than 360°) as shown in Fig. 1(c). We refer to these new patterns as having strong chirality. The new morphological character is inheritable, can be

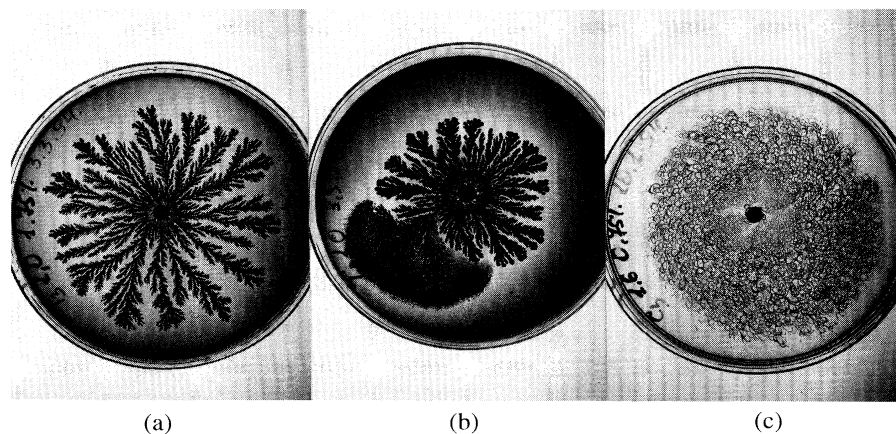


FIG. 1. From branching growth to chiral growth. (a) A typical branching pattern produced by \mathcal{T} morphotype grown on 1 g/l pepton and 1.75% agar concentration. (b) Bursts of \mathcal{C} morphotype from \mathcal{T} morphotype grown on 1 g/l pepton and 1.5% agar concentration. (c) Typical strong chirality exhibited by \mathcal{C} morphotype grown on 1.6 g/l pepton and 0.75% agar concentration.

transferred by an individual bacterium, and is stable for a range of growth conditions, so we refer to it as a distinct morphotype (C morphotype).

The optical microscope observations indicate that during the growth of strong chirality the bacteria move within a well defined envelope [Fig. 2(a)]. The bacteria are long (relative to T morphotype bacteria), and the movement appears correlated in orientation [Fig. 2(b)]. Each branch tip maintains its shape, and at the same time the tips keep twisting with specific handedness while propagating. Electron microscope observations do not reveal any chiral structure on the bacterial membrane [19].

Ben-Jacob *et al.* [16,18] proposed that the growth velocity (the rate of spreading) of the colony is the selective pressure leading to the $T \rightarrow C$ transitions. Indeed, the reverse $C \rightarrow T$ transitions are observed at growth conditions for which T morphotype is faster than C morphotype. The bursts of C morphotype during growth on soft agar are frequent—about 60% of T morphotype colonies grown on suitable substrate show such bursts [21]. Being frequent and in both directions, it is suggestive that the transitions are associated with activation and deactivation of a simple biological property, a property that can lead to dramatic changes in growth patterns.

It is known [6–8] that flagella have specific chirality. We propose that the latter is the origin of the observed chirality. Ordinarily, as the flagella unfold, the bacterium tumbles and ends at a new random angle (relative to the original one). The situation changes for quasi-2D motion (motion in a lubrication layer thinner than the bacterial length). We assume that in this case, of rotation in a plane, the tumbling has a well defined handedness of rotation. Such handedness requires, in addition to the flagella chirality, that the bacteria be able to distinguish between up and down. The growth in an upside-down

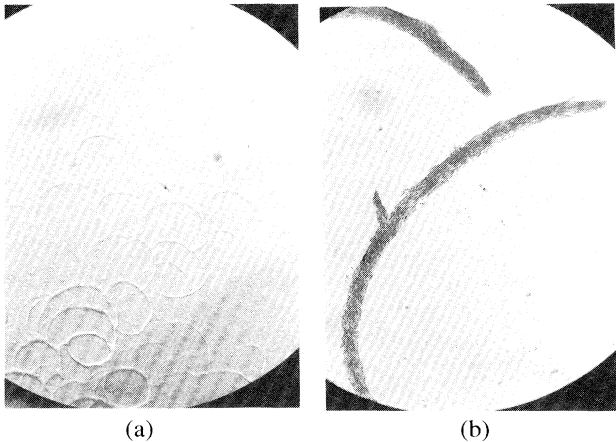


FIG. 2. A close look at the chiral growth. (a) Optical microscope observations 50 times magnification, using reflected light to indicate the three-dimensional structure. (b) Optical microscope observations of a stained colony. 500 times magnification. Each bar is an individual bacterium. The apparent different handedness in comparison with Fig. 1 is a photography artifact—the pictures were taken from behind.

Petri dish shows the same chirality. Therefore, we think that the determination of up vs down is done via the vertical gradient of the nutrients concentration or vertical gradient of signaling materials inside the substrate.

To cause the observed chirality, the rotation of tumbling must be on average smaller than 90° relative to a specific direction, and with a small stochastic part around the average value. We assume that in the case of strong chirality (long bacteria) a bacterium-bacterium coalignment (orientational interaction) limits both the average rotation and its stochastic part. We further assume that the rotation is relative to the local mean orientation of the bacteria.

To test the above, we included the additional assumed features in the communicating walkers model [14]. As before, the bacteria are represented by walkers, each of which should be viewed as a mesoscopic unit (coarse graining over many bacteria). The metabolic state of the i th walker (located at \vec{r}_i) is represented by an “internal energy” E_i . The time evolution of E_i is given by

$$\frac{dE_i}{dt} = E_c \min[c_r, c(\vec{r}_i, t)] - e. \quad (1)$$

It describes an energy increase via food consumption at a constant rate c_r if sufficient food is available [otherwise, the available amount $c(\vec{r}_i, t)$ is consumed], and energy loss at a constant rate e . E_c is a conversion factor from food concentration to energy rate. When there is not enough food for an interval of time (causing E_i to drop to zero), the walker “freezes.” As the walker represents coarse graining, this process represents averaging over the differentiation into immotile states of the individual bacteria, which has a certain probability depending on the level of nutrients. When food is sufficient E_i increases, and when it reaches a threshold t_r the walker divides into two (reproduction).

Diffusion of nutrients is handled by solving the following diffusion equation for the nutrient concentration c :

$$\frac{\partial c(\vec{r}, t)}{\partial t} = D_c \nabla^2 c(\vec{r}, t) - \sum_{\text{active walkers}} \delta(\vec{r} - \vec{r}_i) \min[cr, c(\vec{r}, t)], \quad (2)$$

which includes the consumption of food by the walkers (last term).

To represent the bacterial orientation we assign the new feature of an orientation θ_i to each walker. With every time step, each of the active walkers ($E_i > 0$) performs rotation to a new orientation θ'_i , which is derived from the walker’s previous orientation θ_i by

$$\theta'_i = P(\theta_i, \Phi(\vec{r}_i)) + Ch + \eta. \quad (3)$$

Ch and η represent the new features of rotation due to tumbling. Ch is a fixed rotation, and η is the stochastic part of the rotation (chosen uniformly from the interval $[-\sigma, \sigma]$). $\Phi(\vec{r}_i)$ is the local mean orientation in the neighborhood of \vec{r}_i . P is a projection function that represents the orientational interaction, which acts on each

walker to orient θ_i along the direction $\Phi(\vec{r}_i)$. P is defined by

$$P(\alpha, \beta) = \alpha + (\beta - \alpha) \text{mod} \pi. \quad (4)$$

Once oriented, the walker advances a step d either in the direction θ'_i (forwards) or in the direction $\theta'_i + \pi$ (backwards). Hence the new location \vec{r}'_i is given by

$$\vec{r}'_i = \vec{r}_i + \begin{cases} d(\cos\theta'_i, \sin\theta'_i), & \text{with probability 0.5,} \\ d(-\cos\theta'_i, -\sin\theta'_i), & \text{with probability 0.5.} \end{cases}$$

The movement is confined within an envelope (which is defined on a triangular lattice). That is, the step is not performed if the step $\vec{r}_i \rightarrow \vec{r}'_i$ crosses the envelope. Whenever this is the case, a counter on the appropriate segment of the envelope is increased by 1, and when a segment counter reaches N_c , the appropriate segment of the envelope advances one lattice step.

Next we specify the mean orientation field Φ . To do so, we assume that each lattice cell (hexagonal area unit)

is assigned one value of $\Phi(\vec{r})$, representing the average orientation of the cell. The bacteria in a branch are aligned parallel to the branch's walls, hence Φ may be viewed as the orientation of the nearest wall. The value of Φ is set when a new lattice cell is first occupied (due to the advancement of the envelope) and remains constant (in a more detailed model, the value of Φ may change according to the slow change in the wall's orientation). Its value equals the average over the orientations of the N_c attempted steps, which lead to the occupation of the new lattice cell. In Figs. 3(a) and 3(b) we present a pictorial description of the model [the occupied lattice cells, $\Phi(\vec{r})$, the walkers, and their orientations].

Results of the numerical simulations of the model are shown in Fig. 3(c). These results do capture some important features of the observed patterns: The microscopic twist Ch leads to a chiral morphology on the macroscopic level. The growth is via stable tips, all of which twist with the same handedness and emit sidebranches. The dynamics of the sidebranches' emission in the time evolution of the model is similar to the observed dynamics. The patterns are dense at high pepton levels and become more ramified with decreasing nutrient level. For a given pep-

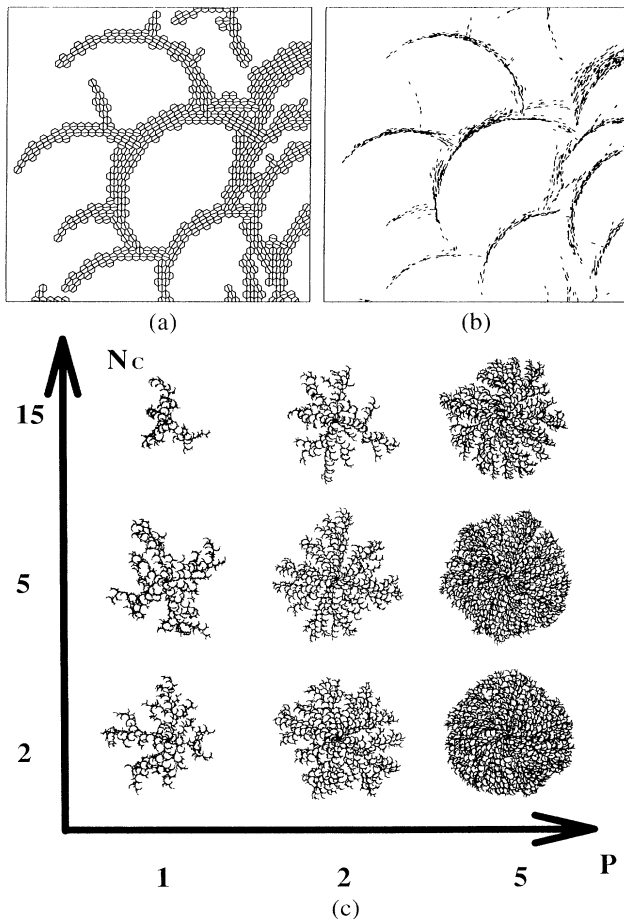


FIG. 3. (a) A close look at a “colony” simulated by the model. Each bar is one walker oriented according to its θ_i . (b) The same as (a) showing the corresponding occupied lattice cells and the mean field orientation of each cell (the bar inside the area). (c) Global patterns simulated by the model as a function of nutrient level P and N_c (the equivalent of pepton level and agar concentration, respectively).

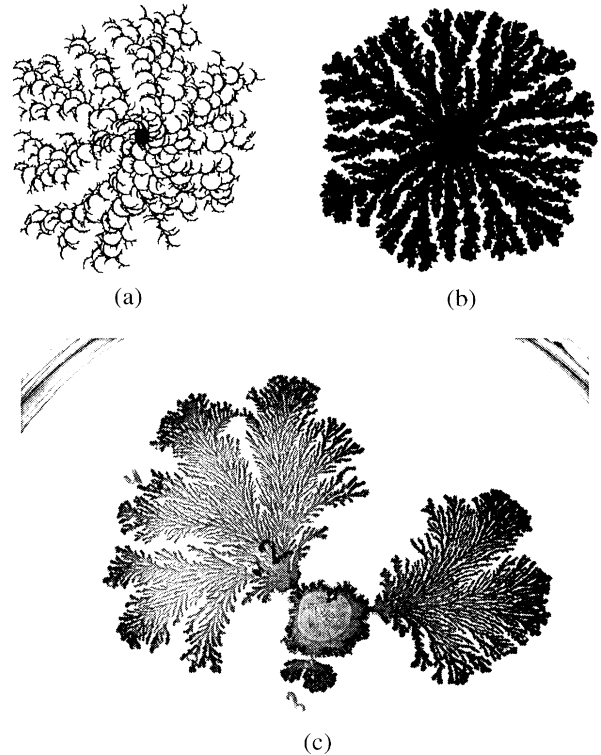


FIG. 4. The effect of the standard deviation of η . (a) Chiral growth for $P = 2$, $N_c = 5$, and $\sigma = 0.035$. (b) Tip-splitting growth of the same model for $P = 8$, $N_c = 15$, and $\sigma = 1.57$. (c) C morphotype exhibits tip-splitting growth for 2.5% agar concentration and 10 g/l pepton level. Optical microscope observations reveal that during tip-splitting growth the bacteria are shorter. As explained in the text, we expect that shorter length of the bacteria corresponds to a larger standard deviation σ .

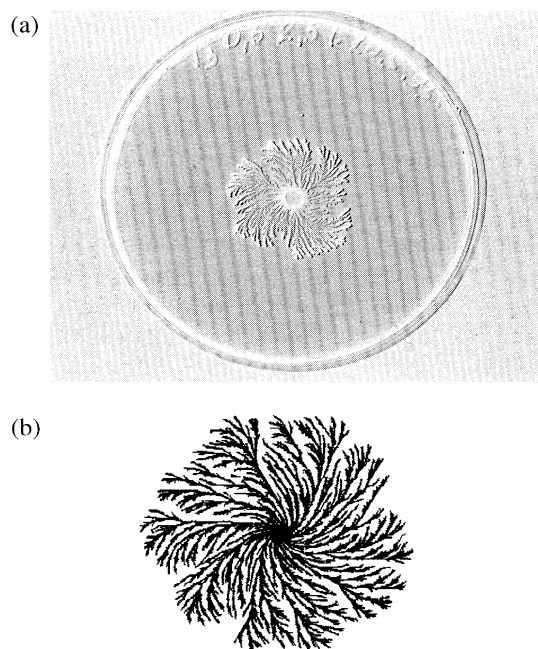


FIG. 5. Weak chirality. (a) Weak chirality exhibited by \mathcal{T} morphotype grown on 4 g/l pepton level and 2.5% agar concentration. (b) Simulation of weak chirality for $P = 3$ and $N_c = 20$. The “dark field” effect is artificial in both (a) and (b).

ton level, the patterns are more ramified for higher agar concentrations. All is in agreement with the experimental observations.

In Fig. 4 we show that for large σ (which corresponds to weak orientation interaction in the case of shorter bacteria) the chiral nature of the pattern disappears and it becomes a branching pattern. This provides a plausible explanation for the branching patterns produced by C morphotype grown on high pepton levels [Fig. 4(c)], as the bacteria are shorter when grown on a rich substrate.

Colonies of \mathcal{T} morphotype grown on a hard substrate (about 2.5% agar concentration) exhibit branching patterns with a global twist of the same handedness, as shown in Fig. 5(a). Similar observations during growth of other bacterial strains have been reported by Matsuyama and co-workers [9,22]. We refer to such growth patterns as having weak chirality, relative to the strong chirality exhibited by the C morphotype.

We propose that, in the case of \mathcal{T} morphotype, it is the high viscosity of the lubrication fluid during growth on hard agar that limits the rotation of tumbling (instead of the bacterium-bacterium coalignment of the C morphotype). We further assume that the rotation is relative to the direction of the gradient of a chemotaxis signaling field (here we used repellent chemotaxis), which serves as a specific direction instead of the local mean orientation field in the case of C morphotype. In Fig. 5(b) we show that inclusion of the above features indeed leads to the observed weak chirality. It also provides a plausible

explanation to the observations of weak chirality by Matsuyama and Matsushita [9] in strains defective in production of lubrication fluid.

To conclude, C morphotype exhibits additional phenomena yet to be explained. We expect most of these phenomena to result from additional interplay of attractant and repellent chemotactic signaling.

We have benefited from conversations with David Gutnick, David Kessler, and Jim Shapiro. We thank Inna Brainis for technical assistance. This research was supported in part by a grant from the G.I.F., the German-Israeli Foundation for Scientific Research and Development, Hungarian Research Foundation Grant No. T4439, United States-Israel Binational Science Foundation (BSF) Grant No. 9200051, and a grant from the Vice President for Research of Tel-Aviv University.

- [1] J. Adler, *Science* **166**, 1588–1597 (1969).
- [2] P. Devreotes, *Science* **245**, 1054–1058 (1989).
- [3] J. A. Shapiro, *Sci. Am.* **258**, No. 6, 62–69 (1988).
- [4] H. C. Berg, *Nature (London)* **254**, 389–392 (1975).
- [5] E. O. Budrene and H. C. Berg, *Nature (London)* **349**, 630–633 (1991).
- [6] M. Eisenbach, *Mol. Microbiol.* **4**, 161–167 (1990).
- [7] J. B. Stock, A. M. Stock, and M. Mottonen, *Nature (London)* **344**, 395–400 (1990).
- [8] C. H. Shaw, *BioEssays* **13**, 25–29 (1991).
- [9] T. Matsuyama and M. Matsushita, *Crit. Rev. Microbiol.* **19**, 117–135 (1993).
- [10] H. Fujikawa and M. Matsushita, *J. Phys. Soc. Jpn.* **58**, 3875–3878 (1989).
- [11] H. Fujikawa and M. Matsushita, *J. Phys. Soc. Jpn.* **60**, 88–94 (1991).
- [12] M. Matsushita and H. Fujikawa, *Physica (Amsterdam)* **168A**, 498 (1990).
- [13] M. Matsushita, J. Wakita, and T. Matsuyama, in *Proceedings of the NATO Advanced Research Workshop on Spatio-Temporal Patterns in Nonequilibrium Complex Systems, Santa-Fe, 1993* (Addison-Wesley, Reading, 1995), pp. 609–618.
- [14] E. Ben-Jacob, O. Shochet, A. Tenenbaum, I. Cohen, A. Czirik, and T. Vichsek, *Nature (London)* **368**, 46–49 (1994).
- [15] E. Ben-Jacob, A. Tenenbaum, O. Shochet, and O. Avidan, *Physica (Amsterdam)* **202A**, 1–47 (1994).
- [16] E. Ben-Jacob, H. Shmueli, O. Shochet, and A. Tenenbaum, *Physica (Amsterdam)* **187A**, 378–424 (1992).
- [17] E. Ben-Jacob, O. Shochet, A. Tenenbaum, and O. Avidan, in *Proceedings of the NATO Advanced Research Workshop on Spatio-Temporal Patterns in Nonequilibrium Complex Systems, Santa-Fe, 1993* (Ref. [13]), pp. 619–634.
- [18] E. Ben-Jacob, A. Tenenbaum, O. Shochet, and O. Avidan, *Physica (Amsterdam)* **202A**, 1–47 (1994).
- [19] E. Ben-Jacob, O. Shochet, A. Tenenbaum, I. Cohen, A. Czirik, and T. Vicsek, *Fractals* **2**, 15–44 (1994).
- [20] J. Schindler and T. Rataj, *Binary* **4**, 66–72 (1992).
- [21] E. Ben-Jacob and I. Cohen (to be published).
- [22] T. Matsuyama, R. M. Harshey, and M. Matsushita, *Fractals* **1**, 302–311 (1993).

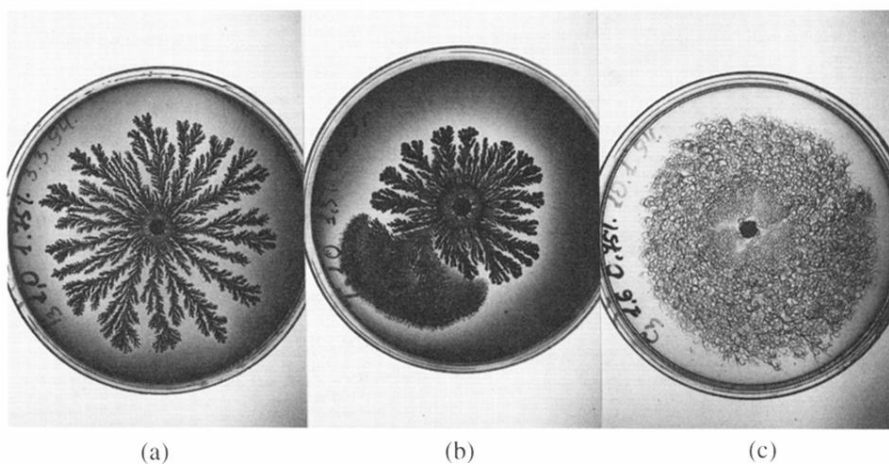


FIG. 1. From branching growth to chiral growth. (a) A typical branching pattern produced by \mathcal{T} morphotype grown on 1 g/l pepton and 1.75% agar concentration. (b) Bursts of \mathcal{C} morphotype from \mathcal{T} morphotype grown on 1 g/l pepton and 1.5% agar concentration. (c) Typical strong chirality exhibited by \mathcal{C} morphotype grown on 1.6 g/l pepton and 0.75% agar concentration.

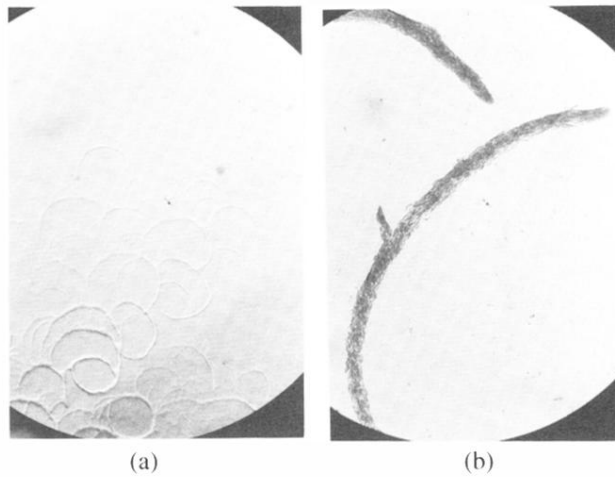


FIG. 2. A close look at the chiral growth. (a) Optical microscope observations 50 times magnification, using reflected light to indicate the three-dimensional structure. (b) Optical microscope observations of a stained colony. 500 times magnification. Each bar is an individual bacterium. The apparent different handedness in comparison with Fig. 1 is a photography artifact—the pictures were taken from behind.

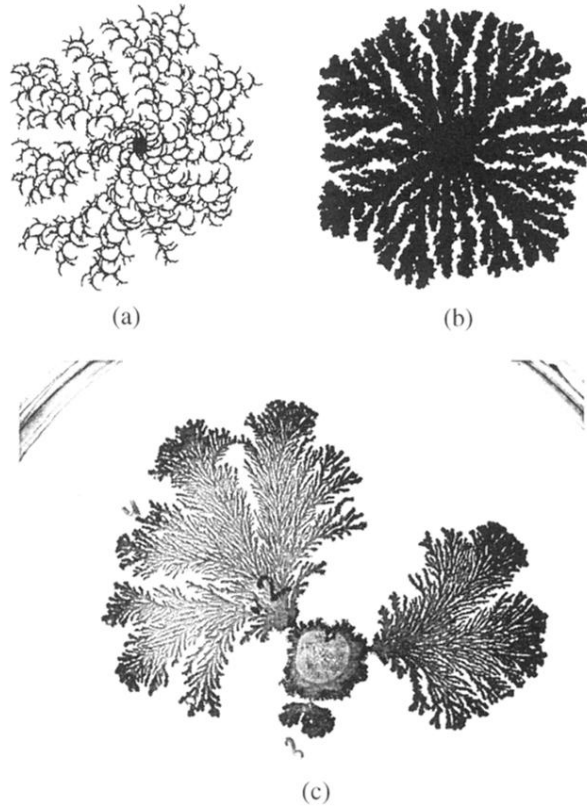


FIG. 4. The effect of the standard deviation of η . (a) Chiral growth for $P = 2$, $N_c = 5$, and $\sigma = 0.035$. (b) Tip-splitting growth of the same model for $P = 8$, $N_c = 15$, and $\sigma = 1.57$. (c) *C* morphotype exhibits tip-splitting growth for 2.5% agar concentration and 10 g/l pepton level. Optical microscope observations reveal that during tip-splitting growth the bacteria are shorter. As explained in the text, we expect that shorter length of the bacteria corresponds to a larger standard deviation σ .

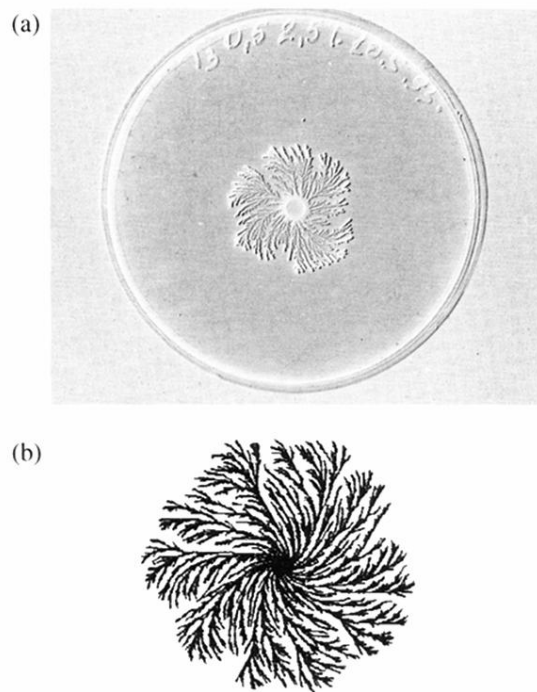


FIG. 5. Weak chirality. (a) Weak chirality exhibited by \mathcal{T} morphotype grown on 4 g/l pepton level and 2.5% agar concentration. (b) Simulation of weak chirality for $P = 3$ and $N_c = 20$. The “dark field” effect is artificial in both (a) and (b).